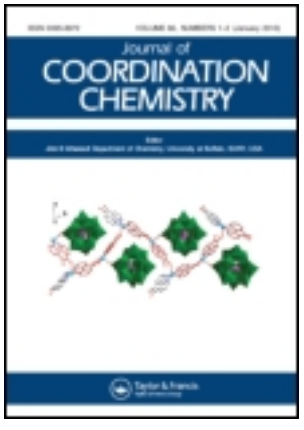

Journal of Coordination Chemistry
Publication details, including instructions for authors and subscription information:
http://www.tandfonline.com/loi/gcoo20

Synthesis, characterization, and DNA-binding of two new Cd(II) complexes with 8-[(2-pyridylmethyl)amino]-quinoline

Jing Lu[ab], Qian Sun[ab], Jun-Ling Li[ab], Wen Gu[ab], Jin-Lei Tian[ab], Xin Liu[ab] & Shi-Ping Yan[a]

[a] Department of Chemistry, Nankai University, Tianjin, P.R. China
[b] Tianjin Key Laboratory of Metal and Molecule Based Material Chemistry, Tianjin, P.R. China

Accepted author version posted online: 07 Aug 2013.Published online: 24 Sep 2013.

To cite this article: Jing Lu, Qian Sun, Jun-Ling Li, Wen Gu, Jin-Lei Tian, Xin Liu & Shi-Ping Yan (2013) Synthesis, characterization, and DNA-binding of two new Cd(II) complexes with 8-[(2-pyridylmethyl)amino]-quinoline, Journal of Coordination Chemistry, 66:18, 3280-3290, DOI: 10.1080/00958972.2013.832228

To link to this article: http://dx.doi.org/10.1080/00958972.2013.832228

Journal of Coordination Chemistry, 2013
Vol. 66, No. 18, 3280–3290, http://dx.doi.org/10.1080/00958972.2013.832228

Synthesis, characterization, and DNA-binding of two new Cd(II) complexes with 8-[(2-pyridylmethyl)amino]-quinoline

JING LU†‡, QIAN SUN†‡, JUN-LING LI†‡, WEN GU†‡, JIN-LEI TIAN†‡, XIN LIU†‡ and SHI-PING YAN*†

†Department of Chemistry, Nankai University, Tianjin, P.R. China
‡Tianjin Key Laboratory of Metal and Molecule Based Material Chemistry, Tianjin, P.R. China

(*Received 27 January 2013; accepted 12 July 2013*)

Two new cadmium(II) complexes, $[Cd_2\mathbf{L}_2Cl_4]$ (**1**) and $[Cd\mathbf{L}_2](ClO_4)_2$ (**2**) {**L** = 8-[(pyridylmethyl) amino]-quinoline}, have been synthesized and characterized by X-ray single-crystal structure analysis. Each neutral **L** is a tridentate terminal ligand. Complex **2** is mononuclear compound whereas **1** is a di-chloride-bridged dinuclear compound. Interactions of the complexes with CT-DNA have been investigated by UV absorption, fluorescence and circular dichroism spectroscopy. Results show that the complexes bind to CT-DNA with moderate intercalation.

Keywords: Cadmium complexes; Di-chloride-bridged; CT-DNA; An intercalative mode

1. Introduction

The development of artificial nucleases plays an important role in biotechnology and drug design [1, 2]. Metal-based synthetic nucleases are important for various applications in nucleic acid and peptide chemistry. Transition metal complexes have been developed as chemical cleavers of nucleic acids and are of interest in the development of artificial nucleases because of their diverse applications in nucleic acids chemistry as footprinting agents, sequence-specific binding, structural probes, and therapeutic agents [3–5]. To find new artificial nucleases that can recognize and cleave DNA effectively, some researchers have designed complexes by changing the metals or ligands [6]. Quinoline and its derivatives are important structural units existing in alkaloids which have important biological activities [7, 8]. Because of the 2 π-stacking ability and potential coordination properties, quinoline subunit has become important in both organic and inorganic chemistry.

To develop artificial nucleases, transition metal complexes containing planar or ring systems are important for interaction with DNA by non-covalent interactions such as electrostatic, intercalative, and groove binding; most attention has centered on metal complexes that are capable of binding DNA by intercalation [9]. The type of central metal, which is responsible for the geometry of complexes, also has significant influence on the

*Corresponding author. Email: yansp@nankai.edu.cn

intercalating ability of DNA. Progress in design of artificial nucleases include Fe^{3+}, Zn^{2+}, Cu^{2+}, Co^{3+} and $Ln^{3+/4+}$; corresponding Cd^{2+} complexes are less reported [10–12].

Due to toxicity of the metal, Cd(II) complexes were seldom investigated [13]. Nevertheless, cadmium complexes with DNA binding ability and antibacterial activities receive more attention [14, 15]. For instance, some Cd(II) complexes exhibit significant antitumor activity on murine melanoma B16 cells and human cervical cancer HeLa cells [16]and show high activity similar to cisplatin with IC_{50} less than 10 μM for some cell lines such as MDA-361, MDA-453, HeLa, etc. [17]. Consequently, investigations of the interaction between the Cd(II) complexes and DNA are important.

In our study, we have synthesized two new cadmium(II) complexes using 8-aminoquinoline. $[Cd_2\mathbf{L}_2Cl_4]$ (**1**) and $[Cd\mathbf{L}_2](ClO_4)_2$ (**2**) {**L** = 8-[(pyridylmethyl)amino]-quinoline} were synthesized and characterized. Both complexes contain extended aromatic π-systems, like metal complexes with tridentate chelating ligands such as N,N-bis(2-pyridylmethyl)amine. Also, we have investigated their interactions with CT-DNA.

2. Experimental

2.1. *Materials*

All reagents and chemicals were purchased from commercial sources and used as received. Calf thymus DNA (CT-DNA) (BR) and ethidium bromide (EB) (AR) were purchased from Sigma. The Tris-HCl buffer solution was prepared using deionized and sonicated triply distilled water.

2.2. *Measurements*

Infrared spectra were recorded as KBr disks using a Bruker TENOR 27 FT-IR spectrometer from 4000 to 400 cm^{-1}. Electronic spectra were measured on a JASCO V-570 spectrophotometer. Fluorescence spectra were obtained from a Cary Eclipse fluorescence spectrophotometer at room temperature. Circular dichroic spectra were studied on a JASCO-J715 CD spectropolarimeter at room temperature. ESI-MS were obtained on an Agilent 6520 Q-TOF LC/MS.

2.3. *Synthesis of complexes*

2.3.1. Preparation of L. 2-(Chloromethyl)pyridine hydrochloride (8.2 g, 50 mM) was dissolved in water (30 mL) in a three-necked flask by stirring and 4 mL aqueous solution of sodium hydroxide (0.01 M) was added dropwise. Several minutes later, ethanolic solution (18 mL) of 8-aminoquinoline (2.88 g, 20 mM) was added in portions. To the above reaction mixture, 6 mL aqueous solution of sodium hydroxide (0.01 M) was added dropwise under nitrogen. After addition, the reaction mixture was stirred for 5 days. An oily gum was formed and extracted with chloroform (3 × 25 mL). Most of the chloroform was evaporated under reduced pressure and the remaining crude product was obtained (Supplementary material, scheme S1).

2.3.2. Preparation of $[Cd_2\mathbf{L}_2Cl_4]$ (1). A solution of **L** (0.0669 g, 0.2 mM) and LiOH (0.0096 g, 0.4 mM) in EtOH:H_2O (1 : 1 v/v, 10 mL) was added dropwise to a solution of

$CdCl_2 \cdot 2.5H_2O$ (0.0685 g, 0.3 mM) in water (10 mL). After 4 h of stirring, the solution was filtered and the filtrate was left in air at room temperature. After several days, colorless well-shaped crystals were obtained and many were suitable for X-ray diffraction studies. Yield = 48% (based on **L**). The crystals were collected by filtration, washed with Et_2O and dried over silica gel. Found (%): C, 42.9; H, 3.0; N, 9.9. Calcd for $C_{30}H_{26}Cd_2Cl_4N_6$ (%): C, 43.0; H, 3.1; N, 10.0. FT-IR (KBr phase): 3144 vs (ν_{N-H}), 2361 s, 1506 m, 1092 s, 830 m, 782 s. The stability of **1** in aqueous solution was investigated by ESI-MS. The major peak at *m/z* 392.01 could be assigned to the molecular ion $[Cd_2\mathbf{L}_2(H_2O)Cl_2]^{2+}$ (figure S1).

2.3.3. Synthesis of $[CdL_2](ClO_4)_2$ (2). This complex was isolated by following the same procedure described for **1**, starting from $Cd(ClO_4)_2 \cdot 6H_2O$ (0.0839 g, 0.2 mM). Yield = 68% (based on **L**). Found: C, 46.2; H, 3.4; N, 10.6 (%). Calcd for $C_{30}H_{26}CdCl_2N_6O_8$ (%): C, 46.1; H, 3.4; N, 10.7. FT-IR (KBr phase): 3246 s (ν_{N-H}), 2360 m, 1606 m, 1097 *versus* 831 m, 787 m. The major peak at *m/z* 619.09 could be assigned to the molecular ion $[Cd\mathbf{L}_2(H_2O)_2–H]^+$ (figure S2).

2.4. *X-ray crystallographic studies*

Determination of the unit cell and data collection were performed with Mo-Kα radiation (λ = 0.71073 Å) on a Bruker Smart 1000 diffractometer equipped with a CCD camera at room temperature (293 K). The structures were solved by direct methods (SHELXS-97) and refined with full-matrix least-squares technique on F^2 using SHELXL-97 [18, 19]. The hydrogens were added theoretically, riding on the concerned atoms and refined with fixed thermal factors. The details of crystallographic data and structure refinement parameters are summarized in table 1.

Table 1. Crystal data and structure refinement for **1** and **2**.

Compound	**1**	**2**
Chemical formula	$C_{30}H_{26}Cd_2Cl_4N_6$	$C_{30}H_{24}CdCl_2N_6O_8$
Formula mass	837.17	779.85
Crystal system	Triclinic	Monoclinic
a/Å	9.819(2)	12.659(3)
b/Å	13.108(3)	17.043(3)
c/Å	13.128(3)	14.703(3)
α/°	84.31(3)	90.00
β/°	86.02(3)	93.19(3)
γ/°	72.08(3)	90.00
Unit cell volume/Å^3	1598.4(6)	3167.2(11)
Temperature/K	293(2)	293(2)
Space group	$P\bar{1}$	*C2/c*
Z	2	4
No. of reflections measured	9223	15,865
No. of independent reflections	5595	3705
R_{int}	0.0561	0.0319
Final R_1 values ($I > 2\sigma$(I))	0.0676	0.0291
Final w$R(F^2)$ values ($I > 2\sigma(I)$)	0.1431	0.0780
Final R_1 values (all data)	0.0974	0.0343
Final $wR(F^2)$ values (all data)	0.1597	0.0801

2.5. *DNA binding studies*

The compounds were dissolved in triply distilled water and DMF [DMF-water, 5% (v/v)]. The DNA binding experiments were performed at room temperature in Tris-HCl/NaCl buffer (50 mM Tris-HCl/1 mM NaCl buffer, pH 7.5) using DMF (5%) solution of **1** and **2**. A solution of CT-DNA in the buffer (pH 7.2) gave a ratio of UV absorbance of 1.8–1.9 at 260 and 280 nm, indicating that the DNA was sufficiently free of protein [20]. The DNA concentration per nucleotide was determined by absorption spectroscopy using the molar extinction coefficient of 6600 M^{-1} cm^{-1} at 260 nm [21].

Absorption titration experiments were performed by maintaining the concentration of the compounds (25 μM) while gradually increasing the concentration of DNA (50 −500 μM). The absorption was recorded after each addition of CT-DNA. Fluorescence measurements were made by using a Varian Cary Eclipse spectrofluorometer. For fluorescence quenching experiments, the cadmium complexes were added to CT-DNA solution treated with EB for 30 min. All samples were excited at 510 nm and emission spectra were recorded at 520–800 nm. The circular dichroism spectra of CT-DNA in the presence or absence of complexes were collected in Tris-HCl buffer (pH = 7.2) containing 50 mM NaCl at room temperature with a JASCO–J715 spectropolarimeter from 230 to 340 nm.

3. Results and discussion

3.1. *The characterization of complexes*

The structure of **1** is depicted in figure 1 and selected bond lengths and angles are listed in table 2. It crystallizes in the triclinic system with space group *P-1*. **1** consists of an uncharged, binuclear cadmium complex. The Cd–Cd distance is 3.675(4) Å and precludes overlap of the vander Waals radii of the two ions [22]. The Cd–Cd distances in other Cd(II) complexes with two bridging chlorides are 3.581–4.077 Å [22–24]. Each cadmium is coordinated with N_3Cl_3

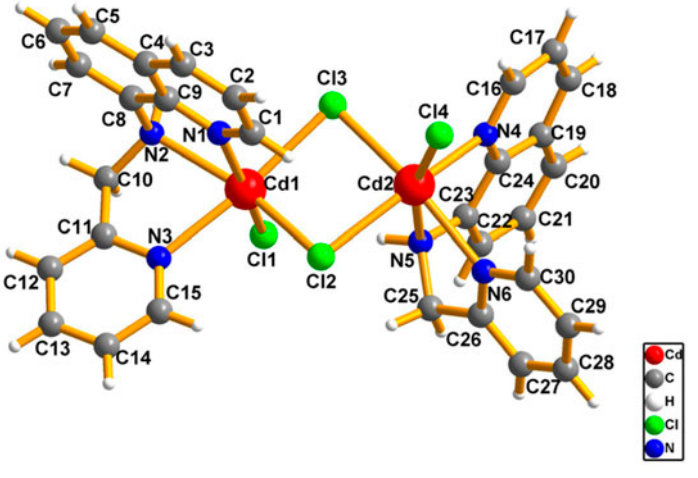

Figure 1. Crystal structure of **1**.

Table 2. Selected bond lengths (Å) and angles (°) for **1**.

Bond distances (Å)			
Cd(2)–N(4)	2.346(7)	Cd(2)–N(6)	2.389(7)
Cd(2)–N(5)	2.433(6)	Cd(2)–Cl(4)	2.472(2)
Cd(2)–Cl(2)	2.640(2)	Cd(2)–Cl(3)	2.652(2)
Cd(1)–Nl(1)	2.366(7)	Cd(1)–N(2)	2.385(7)
Cd(1)–N(3)	2.416(6)	Cd(1)–Cl(2)	2.574(2)
Cd(1)–Cl(1)	2.523(2)	Cd(1)–Cl(3)	2.626(2)
Bond angles (°)			
N(6)–Cd(2)–N(4)	90.6(2)	N(1)–Cd(1)–N(2)	72.2(3)
N(4)–Cd(2)–N(5)	71.2(2)	N(1)–Cd(1)–N(3)	88.6(2)
N(6)–Cd(2)–N(5)	70.5(2)	N(2)–Cd(1)–N(3)	72.1(2)
N(4)–Cd(2)–Cl(4)	100.57(18)	N(1)–Cd(1)–Cl(1)	170.3(2)
N(6)–Cd(2)–Cl(4)	96.19(18)	N(2)–Cd(1)–Cl(1)	99.13(19)
N(5)–Cd(2)–Cl(4)	163.81(17)	N(3)–Cd(1)–Cl(1)	92.91(16)
N(4)–Cd(2)–Cl(2)	159.94(17)	N(1)–Cd(1)–Cl(2)	89.3 (2)
N(6)–Cd(2)–Cl(2)	89.81(17)	N(2)–Cd(1)–Cl(2)	155.74(18)
N(5)–Cd(2)–Cl(2)	90.05(17)	N(3)–Cd(1)–Cl(2)	92.28(17)
Cl(4)–Cd(2)–Cl(2)	99.33(8)	Cl(1)–Cd(1)–Cl(2)	100.15(8)
N(4)–Cd(2)–Cl(3)	84.50(19)	N(1)–Cd(1)–Cl(3)	86.51(16)
N(6)–Cd(2)–Cl(3)	162.26(17)	N(2)–Cd(1)–Cl(3)	103.02(18)
N(5)–Cd(2)–Cl(3)	91.78(18)	N(3)–Cd(1)–Cl(3)	174.00(16)
Cl(4)–Cd(2)–Cl(3)	101.47(8)	Cl(1)–Cd(1)–Cl(3)	91.36(8)
Cl(2)–Cd(2)–Cl(3)	89.09(7)	Cl(2)–Cd(1)–Cl(3)	91.10(7)

donor sets derived from two bridging Cl^-, a pyridine-N, a quinolyl-N and a tertiary amine-N, giving a distorted octahedral geometry. The geometry around cadmium is distorted octahedral. The *cis* bond angles vary from 72.1(2)° to 103.02(18)° for Cd1 and 70.5(2)° to 100.57(18)° for Cd2. The *trans* angles are 155.74(18)°–174.00(16)° for Cd1 and 159.94(17)°–163.83(17)° for Cd2. Of the three main Cartesian axes, the minimum bond angles deviate 24.26° for Cd1 and 20.06° for Cd2 from the ideal value of 180°. Dinuclear cadmium complexes with bridging chlorides are well known and have Cd–Cl (bridging) bond distances ranging from 2.54 to 2.89 Å [23]. Usually the Cd–Cl (terminal) bond distances are shorter than the Cd–Cl (bridging) bond. For **1**, the coordinative bonds between the metal center and the bridging chloride ions (Cd(1)–Cl(2) and Cd(1)–Cl(3)) are longer than the Cd (1)–Cl(1) bond involving the metal center and the non-bridging chloride (2.574(2) and 2.626(2) Å *versus* 2.523(2) Å (table 2)), the same to Cd2 (2.640(2) and 2.52(2) Å *versus* 2.472(2) Å).

The structure of **2** is depicted in figure 2(a) and selected bond lengths and angles are listed in table 3. It crystallizes in the *C2*/c monoclinic space group. For each mononuclear unit, the cadmium is located on the symmetric center. Cd is coordinated to two **L**, giving a distorted octahedral geometry with a N_6 donor set. In fact, **L** is tridentate chelating to Cd(II). The Cd(II)-ligand bond distances (table 3) are similar to those observed in other six-coordinate Cd(II) complexes. The Cd(II)-N(pyridyl) distances (2.3055(18), 2.3847(17), and 2.385(19) Å) resemble those (2.266–2.442 Å) found in most pyridyl-containing six-coordinate Cd(II) complexes. As shown in figure 2(b), in the *ac* plane, the crystal packing geometry of **2** is constituted by two types of intermolecular π–π stacking interactions. One type of intermolecular π–π interaction is between pyridyl rings of **L** and another is between quinolyl rings of **L**. The corresponding plane-plane distances of π–π interaction is 0.3510 nm and 0.3599 nm, respectively.

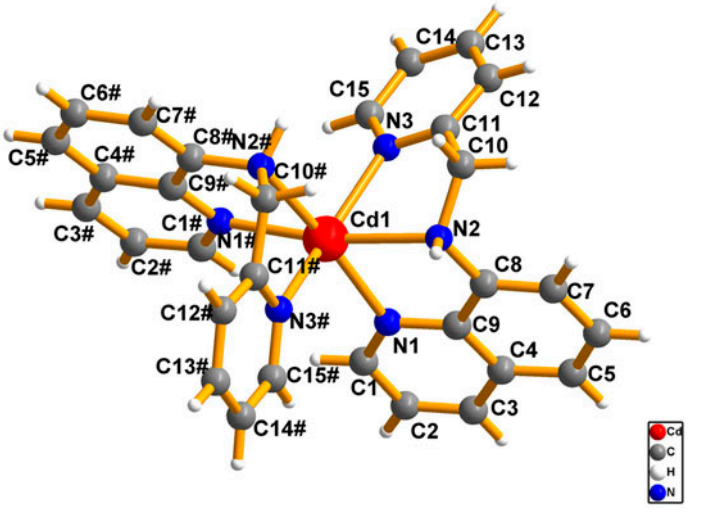

Figure 2a. Crystal structure of **2**.

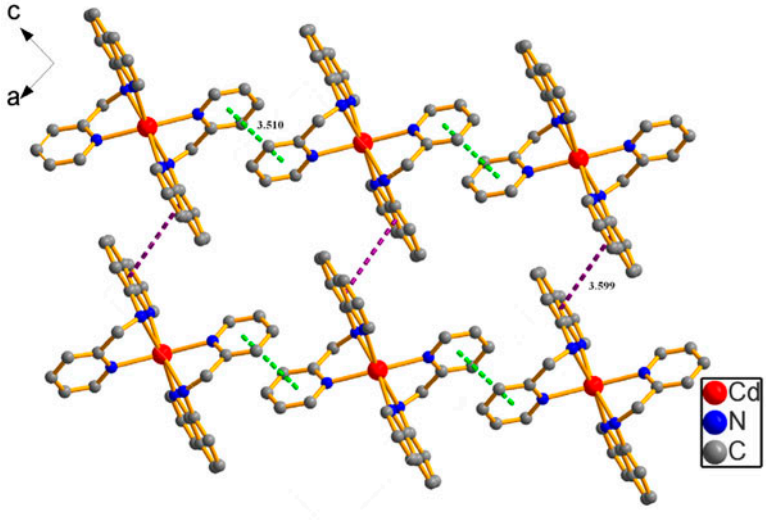

Figure 2b. π–π stacking interactions.

3.2. *DNA-binding modes and affinity studies*

3.2.1. Electronic absorption spectra. Electronic absorption spectroscopy is useful to investigate the interaction of compounds with DNA. Hypochromism with or without a small red or blue shift usually suggests that the compound binds to DNA through intercalation [25]. The results were due to the intercalative mode involving a strong stacking interaction between the planar aromatic chromophore and the base pairs of DNA. After intercalating the base pairs of DNA, the π^* orbital of the intercalated ligand can couple with

Table 3. Selected bond lengths (Å) and angles (°) for **2**.

Bond distances (Å)			
Cd(1)–N(1)	2.3055(18)	Cd(1)–N(1)#1	2.3055(18)
Cd(1)–N(2)	2.3847(17)	Cd(1)–N(2)#1	2.3847(17)
Cd(1)–N(3)	2.3385(19)	Cd(1)–N(3)#1	2.3385(19)
Bond angles (°)			
N(1)–Cd(1)–N(1)#1	110.24(9)	N(1)–Cd(1)–N(3)	93.49(6)
N(1)#1–Cd(1)–N(3)	98.39(6)	N(1)–Cd(1)–N(3)#1	98.39(6)
N(1)#1–Cd(1)–N(3)#1	93.49(6)	N(3)–Cd(1)–N(3)#1	159.16(9)
N(1)–Cd(1)–N(2)#1	170.57(6)	N(1)#1–Cd(1)–N(2)#1	73.97(6)
N(3)–Cd(1)–N(2)#1	94.20(6)	N(3)#1–Cd(1)–N(2)#1	72.67(6)
N(1)–Cd(1)–N(2)	73.97(6)	N(1)#1–Cd(1)–N(2)	170.57(6)
N(3)–Cd(1)–N(2)	72.67(6)	N(3)#1–Cd(1)–N(2)	94.20(6)
N(2)#1–Cd(1)–N(2)	103.20(8)	C(1)–N(1)–Cd(1)	125.27(15)
C(9)–N(1)–Cd(1)	115.59(14)	C(8)–N(2)–Cd(1)	110.42(12)
C(10)–N(2)–Cd(1)	106.13(12)	C(15)–N(3)–Cd(1)	125.98(17)
C(11)–N(3)–Cd(1)	115.41(13)		

Symmetry transformations used to generate equivalent atoms: # $1-x+1, y, -z+½$.

the π orbital of base pairs, thus decreasing the $\pi-\pi^*$ transition energy and resulting in bathochromism. The extent of hypochromism and red shift commonly gives a measure of the strength of DNA binding [26].

For **1** and **2**, the absorption spectral traces with increasing concentration of CT-DNA (0 −160 μM, 280 μM) are shown in figures 3 and 4. The Cd(II) complexes exhibit intense absorption bands in the UV–vis spectra. Peaks at 222 nm for **1** and 224 nm for **2** are attributed to intraligand $\pi-\pi^*$ transition, and addition of increasing amounts of CT-DNA results in hypochromism and an obvious red shift in the UV–vis spectra of the compounds. For **1**, the absorption maximum wavelength shifted from 222 to 226 nm. For **2**, the absorption maximum wavelength shifted from 224 to 230 nm. The Cd(II) complexes exhibit hypochromism of about 25.74 and 47.90% accompanied in the absorption maximum. To determine the binding strength of the complexes with CT-DNA, intrinsic binding constants are K_b were calculated from a nonlinear fitting according to the equation [27, 28]. From the

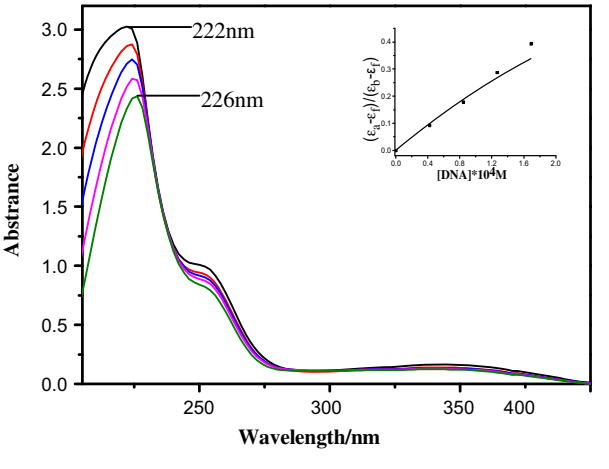

Figure 3. Electronic spectra of **1** in the absence and presence of increasing amount of CT-DNA in 5 mM Tris-HCl/50 mM NaCl buffer (pH = 7.2).

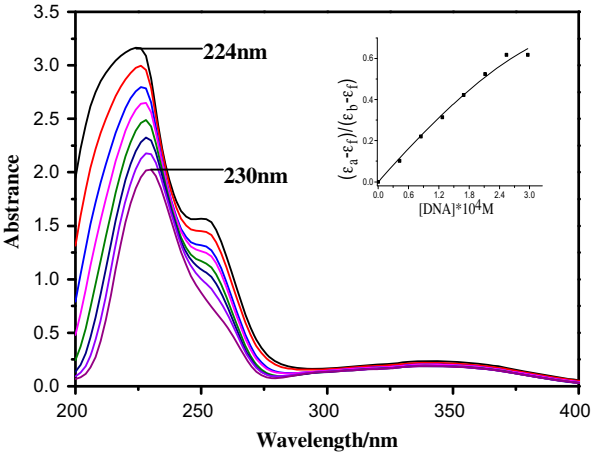

Figure 4. Electronic spectra of **2** in the absence and presence of increasing amount of CT-DNA in 5 mM Tris-HCl/50 mM NaCl buffer (pH = 7.2).

observed spectroscopic changes the values of the intrinsic binding constants K_b ($K_b = 5.03 \times 10^4$ M^{-1} for **1**; $K_b = 2.5 \times 10^5$ M^{-1} for **2**). Compared to the previously reported Cd(II) complexes, K_b for **1** is the same order of magnitude as the binuclear Cd(II) complexes reported by Qiu-Yue Lin [29], which suggest that **1** has medium interaction with DNA; K_b for **2** is a little higher than the previous report of cadmium complex (2.3×10^4 M^{-1}) [30], but lower than that of the classical intercalator EB with DNA. The different binding affinity may be due to steric hindrance.

3.2.2. Fluorescence spectra. To further investigate the interaction of complexes with DNA, steady-state competitive binding experiments were undertaken. EB is a planar cationic dye which is widely used as a sensitive fluorescence probe for native DNA. EB emits intense fluorescence in the presence of DNA due to its strong intercalation between adjacent DNA base pairs [31]. If one complex can replace EB from DNA–bound EB, the fluorescence of the solution will be quenched due to the fact that free EB molecules are readily quenched by the surrounding water molecules [32, 33].

Fluorescence quenching of EB bound to CT-DNA is shown in figures 5(a, b) and 6(a, b). The quenching of EB bound to CT-DNA by both compounds is in agreement with the linear Stern–Volmer equation [34]: $I_0/I = 1 + K[Q]$ which provides further proof that the complexes bind to DNA. The values of apparent DNA binding constant (K_{app}) were calculated using the equation K_{EB} [EB] = K_{app} [complex], where $K_{EB} = 1.0 \times 10^7$ M^{-1} ([EB] = 2.4 μM). $K_{app1} = 0.75 \times 10^5$ M^{-1}; $K_{app2} = 0.93 \times 10^5$ M^{-1}. Such values of binding constants are weaker than the classical apparent DNA binding constant (10^7 M^{-1} [35]), indicating that the interaction of the complexes with DNA are in the medium intercalative mode.

3.2.3. Circular dichroic spectra. CD spectroscopy is sensitive in monitoring the conformational variations of DNA in solution by binding of small molecules. The CD spectrum of CT-DNA consists of a positive band at 275 nm due to base stacking and a negative band at 245 nm due to helicity, characteristic of DNA in the right-handed B form [36]. The

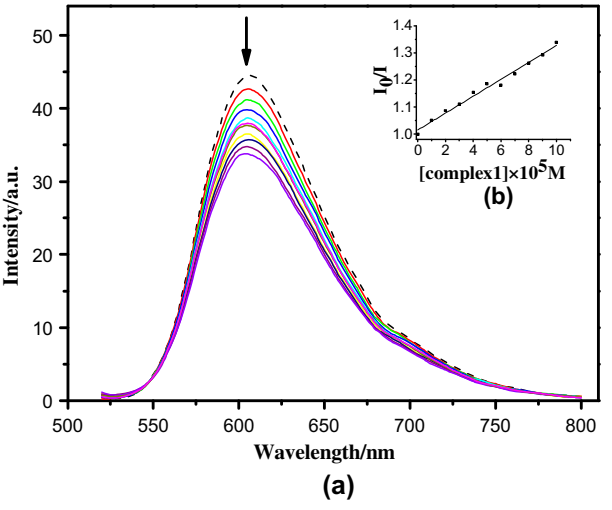

Figure 5. (a) Fluorescence emission spectra (excited at 510 nm) of the CT-DNA-EB system (2.4×10^{-6} ML^{-1} EB, 4.8×10^{-5} ML^{-1} CT-DNA) in the absence and presence of the 1.0×10^{-3} ML^{-1} complex with increasing concentrations from 0 to 100 μM (from top to bottom). (b) The fluorescence quenching curve of EB bound to DNA by **1**.

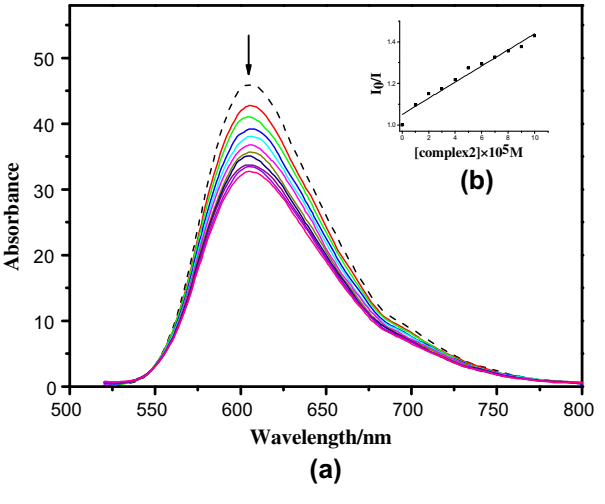

Figure 6. (a) Fluorescence emission spectra (excited at 510 nm) of the CT-DNA-EB system (2.4×10^{-6} ML^{-1} EB, 4.8×10^{-5} ML^{-1} CT-DNA) in the absence and presence of the 1.0×10^{-3} ML^{-1} complex with increasing concentrations from 0 to 100 μM (from top to bottom). (b) The fluorescence quenching curve of EB bound to DNA by **2**.

positive band shows a decrease in intensity with increase in the concentration of complexes (figure 7). These results indicate intercalation for the complexes binding to CT-DNA wherein the complexes stack between the base pairs of DNA, thus unwinding the DNA helix and reducing its stability [37]. From the CD spectrum, binding of the complexes to DNA does not lead to a significant change in the conformation of the secondary structure of DNA.

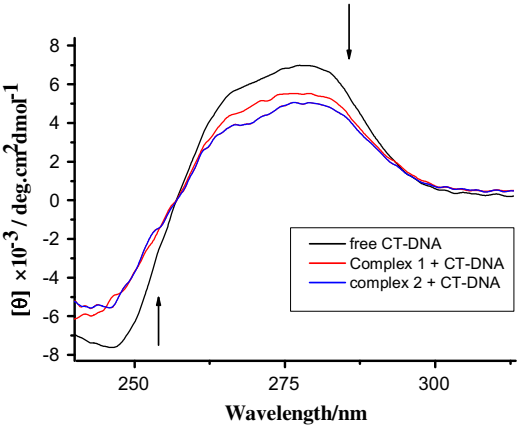

Figure 7. CD spectra of CT-DNA in the buffer solution (Tris-HCl) at 0.6 mM in the absence (black line) and presence of 0.3 mM **1** (red line) and 0.3 mM **2** (blue line). (See http://dx.doi.org/10.1080/00958972.2013.832228 for color version.)

4. Conclusion

Two Cd(II) complexes have been synthesized and structurally characterized. Complex **1** is a di-chloride-bridged dinuclear compound; both Cd complexes are six-coordinate. Complex **2** is a mononuclear species showing a slightly distorted octahedral geometry. The DNA binding properties have been investigated by electronic absorption titration, EB-DNA displacement experiments and circular dichroism studies. Electronic absorption titration provides the fact that the complexes display efficient binding to CT-DNA through intercalation. Fluorescence quenching curve of EB-bound CT-DNA by complexes are in agreement with the classical Stern–Volmer equation, with calculated apparent binding constant values at room temperature (K_{app}) for complexes, suggesting that these complexes are medium intercalators with DNA. In CD spectral technique, **1** and **2** decrease intensity in both the positive and negative bands of DNA, a clear indication of interactions between the complexes and DNA.

Supplementary material

Crystallographic data (excluding structure factors) for the structures in this article have been deposited with the Cambridge Crystallographic Data Center as Supplementary publication CCDC 928804 and 928805. Copies of the data can be obtained, free of charge, on application to the CCDC, 12 Union Road, Cambridge CB2 1EZ, UK. The ESI-MS Experimental figures.

Acknowledgments

This work was supported by the National Natural Science Foundation of China (21171101 and 20771062) and the Tianjin Science Foundation (No. 12JCYBJC13600).

References

[1] M.J. Fernandez, B. Wilson, M. Palacios, M.M. Rodrigo, K.B. Grant, A. Lorente. *Bioconjugate Chem.*, **18**, 121 (2007).
[2] Y. Jin, J.A. Cowan. *J. Am. Chem. Soc.*, **127**, 8408 (2005).
[3] B. Meunier. *Chem. Rev.*, **92**, 1411 (1992).
[4] E.R. Jamieson, S.J. Lippard. *Chem. Rev.*, **99**, 2467 (1999).
[5] N. Berthet, C. Crey-Desbiolles, M. Kotera, P. Dumy. *Chem. Rev.*, **37**, 5237 (2009).
[6] P. Nagababu, S. Satyanarayana. *Polyhedron*, **26**, 1686 (2007).
[7] M. Ozyanik, S. Demirci, H. Bektas, N. Demirbas, A. Demirbas, S.A. Karaoglu. *Turk. J. Chem.*, **36**, 233 (2012).
[8] G.P. Volynets, M.O. Chekanov, A.R. Synyugin, A.G. Golub, O.P. Kukharenko, V.G. Bdzhola, S.M. Yarmoluk. *J. Med. Chem.*, **54**, 2680 (2011).
[9] N.H. Williams, B. Takasaki, M. Wall. *J. Chin. Acc. Chem. Res.*, **32**, 485 (1999).
[10] R. Chen, C.-S. Liu, H. Zhang, Y. Guo, X.-H. Bu, M. Yang. *J. Inorg. Biochem.*, **101**, 412 (2007).
[11] N.A. Illan-Cabeza, R.A. Vilaplana, Y. Alvarez, K. Akdi, S. Kamah, F. Hueso-Urena, M. Quiros, F. Gonzalez-Vilchez, M.N. Moreno-Carretero. *J. Biol. Inorg. Chem.*, **10**, 924 (2005).
[12] X.-F. Ma, D.-D. Li, J.-L. Tian, Y.-Y. Kou, S.-P. Yan. *Transition Met. Chem.*, **34**, 475 (2009).
[13] D.L. Hamilton, L.S. Valberg. *Am. J. Physiol.*, **227**, 1033 (1974).
[14] P. Genova, T. Varadinova, A.I. Matesanz, D. Marinova, P. Souza. *Toxicol. Appl. Pharmacol.*, **197**, 107 (2004).
[15] W.X. Hu, W. Zhou, C. Xia, X. Wen. *Bioorg. Med. Chem. Lett.*, **16**, 2213 (2006).
[16] N.R. Filipović, A. Bacchi, M. Lazić, G. Pelizzi, S. Radulović, D.M. Sladić, T.R. Todorović, K.K. Anđelković. *Inorg. Chem. Commun.*, **11**, 47 (2008).
[17] S. Bjelogrlic, T. Todorovic, A. Bacchi, M. Zec, D. Sladic, T. Srdic-Rajic, D. Radanovic, S. Radulovic, G. Pelizzi, K. Andelkovic. *J. Inorg. Biochem.*, **104**, 673 (2010).
[18] G.M. Sheldrick. *SHELXS-97, Program for the Solution of Crystal Structures*, University of Göttingen, Göttingen (1997).
[19] G.M. Sheldrick. *SHELXL-97, Program for the Refinement of Crystal Structures*, University of Göttingen, Göttingen (1997).
[20] J. Marmur. *J. Mol. Biol.*, **3**, 208 (1961).
[21] M.E. Reichmann, S.A. Rice, C.A. Thomas, P. Doty. *J. Am. Chem. Soc.*, **37**, 3047 (1954).
[22] A. Bondi. *J. Phys. Chem.*, **68**, 441 (1964).
[23] Y. Kang, S.-H. Moon, J. Chul Byun. K-M. Park. *Bull. Korean Chem. Soc.*, **31**, 3017 (2011).
[24] S.M. Berry, D.C. Bebout. *Inorg. Chem.*, **44**, 27 (2005).
[25] S.A. Tysoe, R.J. Morgan, A.D. Baker, T.C. Strekas. *J. Phys. Chem.*, **97**, 1707 (1993).
[26] C. Tu, Y. Shao, N. Gan, Q. Xu, Z. Guo. *Inorg. Chem.*, **43**, 4761 (2004).
[27] J.D. McGhee, P.H. von Hippel. *J. Mol. Biol.*, **86**, 469 (1974).
[28] M.T. Carter, M. Rodriguez, A.J. Bard. *J. Am. Chem. Soc.*, **111**, 8901 (1989).
[29] F. Zhang, X.-L. Zheng, Q.-Y. Lin, P.-P. Wang, W.-J. Song. *Inorg. Chim. Acta*, **394**, 85 (2013).
[30] H.L. Wu, K.T. Wang, F. Kou, F. Jia, B. Liu, J.K. Yuan, Y. Bai. *J. Coord. Chem.*, **65**, 2676 (2011).
[31] F.J. Meyer-Almes, D. Porschke. *Biochemistry*, **32**, 4246 (1993).
[32] B.C. Baguley, M. Le Bret. *Biochemistry*, **23**, 937 (1984).
[33] R.F. Pasternack, M. Caccam, B. Keogh, T.A. Stephenson, A.P. Williams, E.J. Gibbs. *J. Am. Chem. Soc.*, **113**, 6835 (1991).
[34] J.R. Lakowicz, G. Weber. *Biochemistry*, **12**, 4161 (1973).
[35] M. Cory, D.D. McKee, J. Kagan, D.W. Henry, J.A. Miller. *J. Am. Chem. Soc.*, **107**, 2528 (1985).
[36] A.I. Meyers, R.A. Amos. *J. Am. Chem. Soc.*, **102**, 872 (1980).
[37] S. Mahadevan, M. Palaniandavar. *Bioconjugate Chem.*, **7**, 138 (1996).